Original Article

Characterization of the BH1406 non-small cell lung cancer (NSCLC) cell line carrying an activating SOS1 mutation

Gerhard Hamilton[1], Sandra Stickler[1], Mikhail Ermakov[2], Marie-Therese Eggerstorfer[1], Francesca Paola Nocera[1,3], Martin Hohenegger[1], Lukas Weigl[4], Maximilian Johannes Hochmair[5], Karl Kashofer[2]

[1]Institute of Pharmacology, Medical University of Vienna, Vienna, Austria; [2]Diagnostic and Research Institute of Pathology, Medical University of Graz, Graz, Austria; [3]Department of Veterinary Medicine and Animal Production, University of Naples "Federico II", Naples, Italy; [4]Department of Special Anaesthesia and Pain Therapy, Medical University of Vienna, Vienna, Austria; [5]Karl Landsteiner Institute for Lung Research and Pulmonary Oncology, Klinik Floridsdorf, Vienna, Austria

Contributions: (I) Conception and design: G Hamilton, MJ Hochmair; (II) Administrative support: L Weigl, M Hohenegger; (III) Provision of study materials or patients: MJ Hochmair; (IV) Collection and assembly of data: S Stickler, M Ermakov, MT Eggerstorfer, FP Nocera, M Hohenegger, K Kashofer; (V) Data analysis and interpretation: S Stickler, M Ermakov, MT Eggerstorfer, FP Nocera, M Hohenegger, K Kashofer; (VI) Manuscript writing: All authors; (VII) Final approval of manuscript: All authors.

Correspondence to: Prof. Dr. Gerhard Hamilton, PhD. Institute of Pharmacology, Medical University of Vienna, Währinger Strasse 13A, A-1090 Vienna, Austria. Email: gerhard.hamilton@meduniwien.ac.at.

Background: Approximately 30% of the non-small cell lung cancer (NSCLC) patients which harbor no recognizable oncogenic driver mutation are not eligible for targeted therapy. Functional drug screening of tumor cells helps to identify susceptible drug targets not recognized by gene panels for targeted mutation analysis. The aim of this study is to characterize the BH1406 cell line carrying an activating SOS1 mutation and to check its sensitivity to cognate inhibitors.

Methods: The NSCLC cell line BH1406 was established from a pleural effusion and found to be sensitive to the SOS1 inhibitor BAY-293 in initial viability screenings. Since in a limited next-generation sequencing (NGS) lung cancer mutation panel no driver could be detected, the patient underwent chemotherapy with poor outcome. This cell line was further characterized by exome sequencing, SOS1 Western blotting, comparison of two-dimensional (2D) and three-dimensional (3D) chemosensitivity assays and phosphoprotein arrays.

Results: In whole-exome sequencing (WES) the SOS1 mutation P481delinsLFFL, positioned near the known P478L activating mutation was detected. Besides BAY-293, BH1406 cells proved to be sensitive to the SOS1 inhibitors MRTX0902 and BI-3406. The sensitivity of BH1406 cells to BI-3406 was increased under 3D conditions compared to 2D cultures. Western blot phosphoprotein arrays revealed reduced phosphorylation of CREB, GSK3, CHK-2 and STAT3 in BH1406 by BAY-293 treatment in 2D culture. In 3D conditions, cells switched from GSK3α to elevated ERK1/2 signaling, again blocked by the SOS1 inhibitor BAY-293. Similar results were obtained for the SOS1 inhibitors MRTX0902 and BI3406. Additionally, the PI3K inhibitor dactolisib, the GSK-3 inhibitor BI-5521 as well as the bromodomain protein-directed PROTAC ARV-771 inhibited the growth of BH1406 cells significantly and showed synergistic interaction with BAY-293. Furthermore, Western blots demonstrated reduced expression of SOS1 and MYC proteins in response to BAY-293 treatment.

Conclusions: The rare SOS1 P481delinsLFFL mutation in lung cancer may be targetable with corresponding inhibitors, alone or in combination with GSK3/PI3K/BET inhibitors. BH1406 cells represent a novel cellular model suitable for the molecular characterization of SOS1 druggability. Such rare oncogenic driver genes are not included in standard NGS panels and need to be detected by expanded assays like WES.

Keywords: Non-small cell lung cancer (NSCLC); SOS1; mutation; SOS1 inhibitors; cell signaling

Submitted Jul 04, 2024. Accepted for publication Sep 29, 2024. Published online Nov 28, 2024.
doi: 10.21037/tlcr-24-570
View this article at: https://dx.doi.org/10.21037/tlcr-24-570

Introduction

Lung adenocarcinomas are marked by recurrent mutations in the receptor tyrosine kinase (RTK)/rat sarcoma (RAS)/rapidly accelerated fibrosarcoma (Raf) pathway, with up to 75% of cases harboring mutations in known driver genes (1). Recent analysis of whole-exome sequencing (WES) data in non-small cell lung cancer (NSCLC) cohorts has identified SOS1 alterations in rare NSCLC cases which lack canonical oncogenic mutations (2). In detail, WES of 660 lung adenocarcinoma cases identified 242 samples lacked any identifiable oncogenic drivers that are currently targetable (3). However, these samples harbored recurrent mutations linked to the RTK/RAS/Raf pathway, such as ARHGAP35, RASA1, SOS1 and VAV1 (3). Moreover, in the recent analysis from The Cancer Genome Atlas (TCGA), SOS1 mutations were confirmed in 1% of NSCLC samples, 1% of uterine carcinomas, and <1% in other cancers (4).

SOS1 is an activating guanine nucleotide exchange factor (GEF) for RAS proteins facilitating the exchange of guanosine diphosphate (GDP) for guanosine triphosphate (GTP) (5,6). The SOS1 protein consists of multiple domains: a Dbl homology (DH) domain with potential RAC guanine nucleotide exchange factors (GEF) activity, a pleckstrin homology (PH) domain that, together with the DH domain, forms an autoinhibitory region, a RAS exchange motif (REM) that functions as an allosteric activator, and a CDC25-homologous catalytic domain (7-9). In lung adenocarcinomas, mutations in the *SOS1* gene occur across all its domains, with a notable hotspot mutation at the Asn233 residue.

The transcriptional profile of SOS1 N233Y cells showed an increase in KRAS and MYC target gene expression, aligning with SOS1's role as a regulator of RAS and the capacity of RAS signaling to stabilize MYC protein (10,11). Cells with different SOS1 mutations, such as the recurrent N233Y mutation along with D309Y, P478L, and G604V mutations, exhibited a significantly higher colony formation *in vitro* compared to wildtype cells (2). Ectopic expression of NSCLC-derived SOS1 mutations induce anchorage-independent cell growth *in vitro* and tumor formation *in vivo*. These mutations result in increased activation of the RAS pathway, which can be mitigated by mutations that interfere with either the RAS GEF or the putative RAC GEF activity of SOS1 (2). Transcriptional profiling of NIH-3T3 cells transfected with SOS1 N233Y has revealed an increased expression of MYC target genes and others connected to RAS transformation (2). Moreover, the acute myeloid leukemia cell line OCI-AML5, harboring the SOS1 N233Y mutation proved the role of SOS1 as an oncogene promoting survival and sensitivity to MEK inhibition (2).

Noonan syndrome (NS) is a relatively common disorder with variable clinical features, including reduced growth after birth, distinctive facial dysmorphism, and congenital heart defects (CHDs) (12,13). NS is a genetically heterogeneous disorder caused by overactivation of the RAS-MAPK pathway, while a high proportion of cases is due to missense mutations in SOS1 (14-16). Mutation scanning of the entire SOS1 coding sequence revealed 33 variants, such as 16 novel missense changes as well as in-frame indels, of pathological significance (17). Two clusters were anticipated to increase SOS1's recruitment to the

Highlight box

Key findings

- The BH1406 non-small cell lung cancer (NSCLC) line was isolated from a pleural effusion and exhibited high sensitivity to the SOS1 inhibitor BAY-293 in the absence of any other detectable driver mutation. By whole-exome sequencing (WES), the novel P481delinsLFFL SOS1 activating mutations was detected.

What is known and what is new?

- Rare SOS1 oncogenic mutations have been reported in diverse cancer entities and shown to stimulate cancer colony formation *in vitro* and tumors *in vivo*.
- The BH1406 line constitutes a malign NSCLC SOS1-driven cancer cell line that could be inhibited *in vitro* by SOS1 inhibitors under two-dimensional and three-dimensional growth conditions. Inhibitors of CREB, GSK3α/β and CHECK2 show synergistic activity with the BAY-293 SOS1 inhibitor.

What is the implication, and what should change now?

- Rare oncogenic mutations in NSCLC may not be covered by routine test panels for the most frequently altered drivers, such excluding patients from novel targeted therapies. Although such causative genetic alterations can be tested *in vitro* by exposure of tumor cells, WES should be performed for additional mutations and help to guide therapy.

plasma membrane and to enhance its activity in signal transduction. Germline SOS1 mutations are also found in other Rasopathies, such as hereditary gingival fibromatosis type I (18). Mutations of SOS1 in these genetic diseases, are presumed to be gain of function genetic alterations.

Although the oncogenic role of SOS1 mutations has been demonstrated in several tumor entities, possible druggability of SOS1 mutant variants is now progressing (19). Our research group is focusing on functional drug testing in patient-derived NSCLC cell lines derived from pleural effusions. For the detection of relevant SOS1 mutations for clinical diagnosis, WES may be required to detect rare activating mutations. We previously observed that the NSCLC cell line BH1406 had high chemosensitivity to the SOS1 inhibitor BAY-293 despite lacking mutations in the KRAS oncogene (unpublished observation). In the present study we aimed at the characterization of the oncogenic SOS1 mutation in BH1406 as well as the activity of various SOS1 inhibitors. We present this article in accordance with the MDAR reporting checklist (available at https://tlcr.amegroups.com/article/view/10.21037/tlcr-24-570/rc).

Methods

Pleural effusion

This study was conducted in accordance with the Declaration of Helsinki (as revised in 2013). Thoracocentesis of pleural effusions is routinely performed for NSCLC patients and the samples were obtained according to the guidelines set forth in the Ethics Approval EK-21-210-1221 granted by the Ethics Committee of the Medical University of Vienna, Vienna, Austria, including informed consent of the patients. The same protocol was valid for the establishment of the cell line BH1406 from a female NSCLC patient.

Cell culture

Pleural effusions were centrifuged and the cells were washed with tissue culture medium RPMI-1640 (R8758, Sigma-Aldrich, St. Louis, MO, USA) that was supplemented with 10% fetal bovine serum (Eximus, Catus Biotech, Tutzing, Germany) and antibiotics (penicillin-streptomycin; Sigma-Adrich). Cell lines were established under tissue culture conditions (5% CO_2, 37 ℃) and aliquots frozen in liquid nitrogen. The MycoStrip® test (InvivoGen, Tolouse, France) provided evidence for the absence of mycoplasma. Cells were counted via LUNA cell counter (Biozym, Vienna, Austria) and regularly split by trypsinization. To allow for a comparison of two-dimensional to three-dimensional growth of cells, poly (2-hydroxyethylmethacrylat) (pHEMA) (P3932, Sigma-Aldrich) was used to coat 6-well plates (Greiner Bio-One GmbH, Kremsmuenster, Austria) for prevention of cell attachment (20).

Cytotoxicity test

Cells (1×10^4) were distributed to the wells of 96 microtiter plates (Techno Plastic Products AG, Trasadingen, Switzerland) in 100 µL medium with 10 twofold dilutions of the compounds. BAY-293 was purchased from Sigma Aldrich (SML2703). MRTX0902, CHIR-98014, Dactolisib, ARV-771 were purchased from Selleck Chemicals (Catalog No. E1183, Catalog No. S2745, Catalog No. S1009, Catalog No. S8532, Houston TX, USA). BI-3406 and BI-5521 were obtained from Boehringer-Ingelheim (openME, Ingelheim, Germany). All compounds were used as 10 mM stock solutions in dimethyl sulfoxide (DMSO). Viability of the cells was determined after 4 days incubation in tissue culture using a modified 3-(4, 5-dimethylthiazolyl-2)-2, 5-diphenyltetrazolium bromide (MTT) test kit (EZ4U, Biomedica, Vienna, Austria). Tests were performed in triplicate with 10 dilutions and three independent repetitions. The resulting data was calculated with Origin 9.1 software (OriginLab, Northampton, MA, USA).

Western blot analysis

Following incubation with different agents, cells were lysed in RIPA buffer consisting of 50 mM Tris-HCl (pH 8.0), 150 mM NaCl, 0.1% SDS, 1% NP-40, 10 mM glycerol phosphate, 1 mM aprotinin, 1 mM leupeptin, 1 mM Pefabloc (Sigma-Aldrich), 1 mM NaVO3, 5 mM NaF, sonicated and centrifuged (30,000 × g, 4 ℃, 40 min). Aliquots of the supernatant (25–30 µg) were separated on 10% SDS polyacrylamide gels and transferred to nitrocellulose membranes for exposure to primary antibodies against GAPDH (D16H11), c-Myc (E5Q6W) and SOS1 (D3T7T) from Cell Signaling Technology (Leiden, The Netherlands). The appropriate HRP-conjugated secondary antibodies (anti-rabbit IgG, HRP-linked antibody #7074, Cell Signaling Technology, Inc., MA, USA) were used to allow specific detection of the protein of interest by ECL Plus detection system (GE Healthcare, Bucks, UK). The intensities of the protein

bands were measured with a C-Digit blot scanner and normalized to controls (Li-Core, Bad Homburg, Germany).

Western blot arrays

Relative phosphorylation of proteins was determined using a Proteome Profiler Human Phospho-Kinase Array Kit (ARY003C, R&D Systems, Minneapolis, MN, USA) according to the manufacturer's instructions. Experiments were performed in duplicate and the six reference spots provided on each membrane were used to calibrate the individual chemoluminescence intensities. The arrays were evaluated using Quickspot (Ideal Eyes System, Bountiful, UT, USA) and Origin 9.1 software.

WES and variant calling

For WES, next-generation sequencing (NGS) libraries were prepared using SureSelect Human All Exon V8 kit (Agilent, Santa Clara, CA, USA) and sequenced on Illumina NovaSeq6000 (Illumina, San Diego, CA, USA) according to the manufacturers' protocols. Data was analyzed using open-source software, which included alignment to the reference genome (HG38), deduplication and variant calling using Genome Analysis Toolkit (GATK) (Broad Institute, Cambridge, MA, USA) package (Version 4.4.0.0, Apache 2.0 license) (https://github.com/broadinstitute/gatk). Somatic variants were called using Mutect2 (Version 4.1.0.0, Broad Institute, Cambridge, MA, USA) (21), Strelka2 (Version 2.9, Illumina) (22) and VarDict (https://github.com/AstraZeneca-NGS/VarDict) (23). Called variants were annotated using Variant Effect Predictor (VEP) (https://www.ensembl.org) (24). Only somatic variants with >10 reads, allelic frequency in population <1% and variant allele frequency (VAF) >10% were considered in this study.

Statistical analyses

The MTT experiments were performed at least three times and carried out in duplicate. Data was then presented as mean ± standard deviation (SD), if not otherwise stated. Student's *t*-test was used to compare two different treatments. A value of $P<0.05$ was considered to be statistically significant. For Western blot arrays pixel values were normalized to ensure comparability and statistical significances $P<0.05$ were calculated by *t*-tests. The Chou-Talalay method (Calcusyn software, Version 2.0, BIOSOFT, Acropolis Computers Ltd, Cambridge, UK) was used to evaluate drug combinations. Combination index (CI) values <0.1–0.9 were considered synergistic, 0.9–1.10 as additive and 1.1–>10 as antagonistic effects.

Results

Genomic analysis of the BH1406 NSCLC cell line

Oncomine Focus NGS analysis of parental BH1406 tumor did not reveal any actionable genetic alteration. WES of the patient-derived BH1406 cell line was performed to identify possible driver mutations not covered in the routine diagnostic panel. The clonal SOS1 P481delinsLFFL (VAF: 48.08%) mutation, which has not been previously reported was found (Figure S1). Additional pathogenic and likely pathogenic mutations were detected upon screening of genes included in Cancer Gene Census [Catalogue of Somatic Mutations in Cancer (COSMIC)]: STK11 P217Rfs*66 (VAF: 99.7%), TP53 P278S (VAF: 99.8%), ARID2 Q920* (VAF: 99.8%) and FCGR2B R72Gfs*55 (VAF: 33.5%) (25,26). Moreover, the following somatic mutations of uncertain significance were detected in COSMIC genes: DNMT3A A254T (VAF: 32.70%), PTPN13 R923G (VAF: 67.60%), LARP4B N386K (VAF: 44.30%), ETNK1 P6Rfs*140 (VAF: 59.80%), and KEAP1 L175Wfs*55 (VAF: 99.90%) (see Table S1).

BAY-293 reduces expression of SOS1 and MYC in BH1406

BAY-293 treated BH1406 cells were analyzed in Western blots for SOS1 and MYC expression and revealed a significant decrease of both expression levels (*Figure 1*) (27).

The cell line BH1406 was found to be more sensitive to BAY-293 compared to KRAS wildtype BH1395 (*Figure 2*). BH1406 cells were seeded in the absence and presence of pHEMA pretreated wells to allow 2D and 3D spheroidal growth. *Figure 3* demonstrates that sensitivity of BH1406 towards the SOS1 inhibitor BI-3406 differs substantially depending on 2D or 3D conditions (28). With a half maximal inhibitory concentration (IC50)-value of 1.12 and 1.04 µM BAY-293 was the most potent compound to inhibit viability in the absence and presence of pHEMA, respectively. Although, BI-3406 inhibited cell viability with similar potency under pHEMA coated growth conditions, the efficacy was limited to 60%. Similarly, MRTX0902 was not able to reduce viability in a pHEMA dependent manner (29).

However, controls of BH1406 pre-cultured with pHEMA showed significant reduction in the amount of

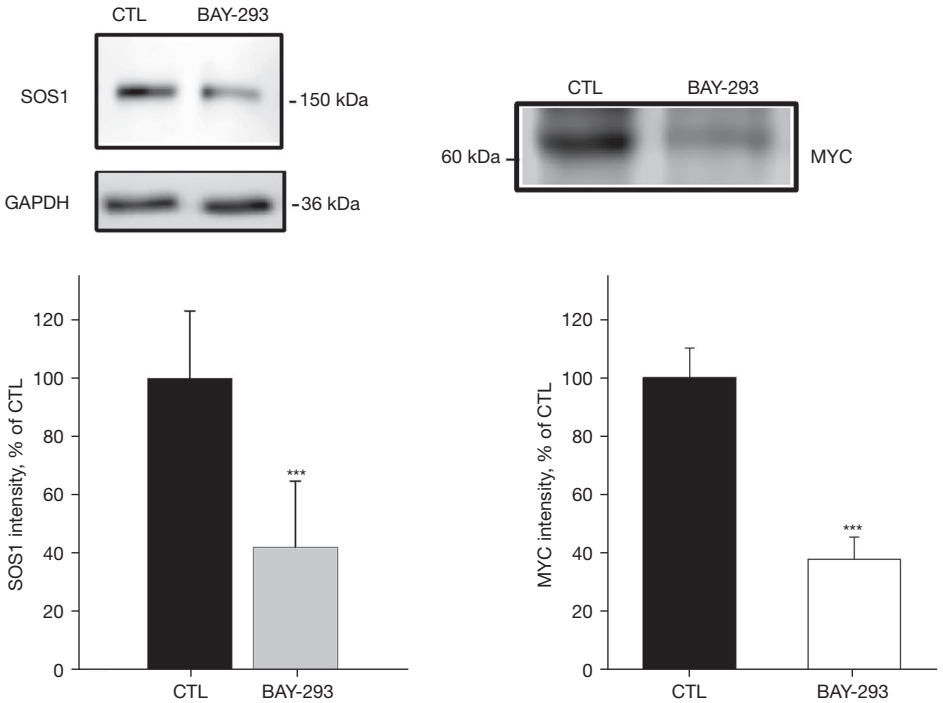

Figure 1 SOS1 (left) and MYC (right) reduction by BAY-293 treatment in BH1406 lung cancer cells. Representative Western blots from BH1406 lung cancer cells (CTL) treated with 0.5 µM BAY-293 for 72 hours are depicted, using specific antibodies for SOS1 and GAPDH as a loading control. Six Western blots were quantified, and intensities normalized to the controls. The bar diagram shows the mean ± SD (***, P<0.001 versus control; Student's *t*-test). CTL, control; SD, standard deviation.

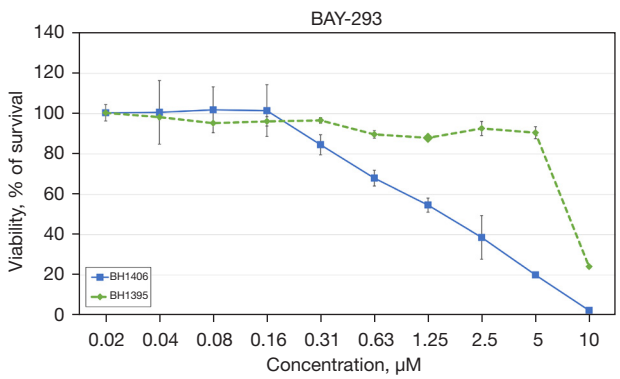

Figure 2 Cytotoxicity assays using an initial concentration of 10 µM BAY-293 against BH1406 and KRAS wildtype BH1395. Data shown are mean values ± SD for 10 two-fold dilutions of the compounds. The IC50-value for BH1406 treated with BAY-293 is 1.12 µM, and BH1395 is 8.06 µM. SD, standard deviation; IC50, half maximal inhibitory concentration.

phosphorylated CREB, GSK-3α/β, checkpoint kinase 2 (Chk-2) and STAT3, while extracellular signal-regulated kinase 1/2 (ERK1/2) was elevated. There were significant reductions of CREB, GSK-3α/β, Chk-2 and STAT3 phosphorylation relatively to controls after treatment with all SOS1 inhibitors and independently of a pre-cultivation of the cells with exception of Chk-2 and BI-3406 (*Figure 4A-4C*). The complete analyses of phosphoproteins comprising all phosphorylation sites are presented in Figures S2,S3.

After pre-cultivation of the cells on pHEMA, ERK 1/2 showed a significant increase of its phosphorylation (*Figure 4A-4C*). In response to the treatment with BAY-293, 2D cells revealed no difference in phosphorylation but the 3D cells on pHEMA showed a significant decrease in its phosphorylation (*Figure 4A*). However, after treatment with the SOS1 inhibitors MRTX0902 and BI-3406 BH1406 2D and 3D cells likewise showed a significantly lower

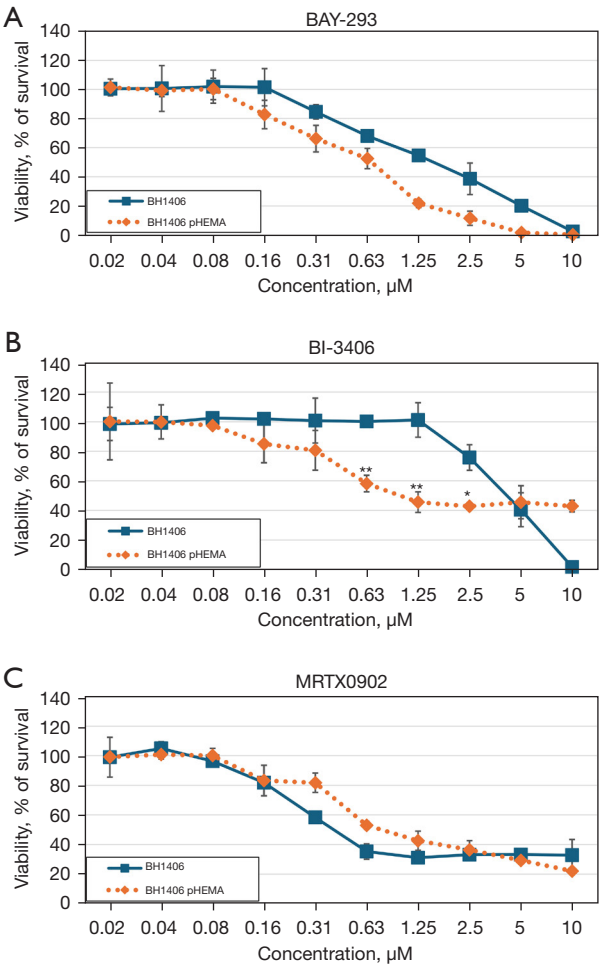

Figure 3 Cytotoxicity assays using an initial concentration of 10 µM (A) BAY-293, (B) BI-3406 and (C) MRTX0902 against BH1406 and BH1406 pre-cultured on 6-well plates coated with pHEMA. Data shown are mean values ± SD for 10 two-fold dilutions of the compounds. SD, standard deviation.

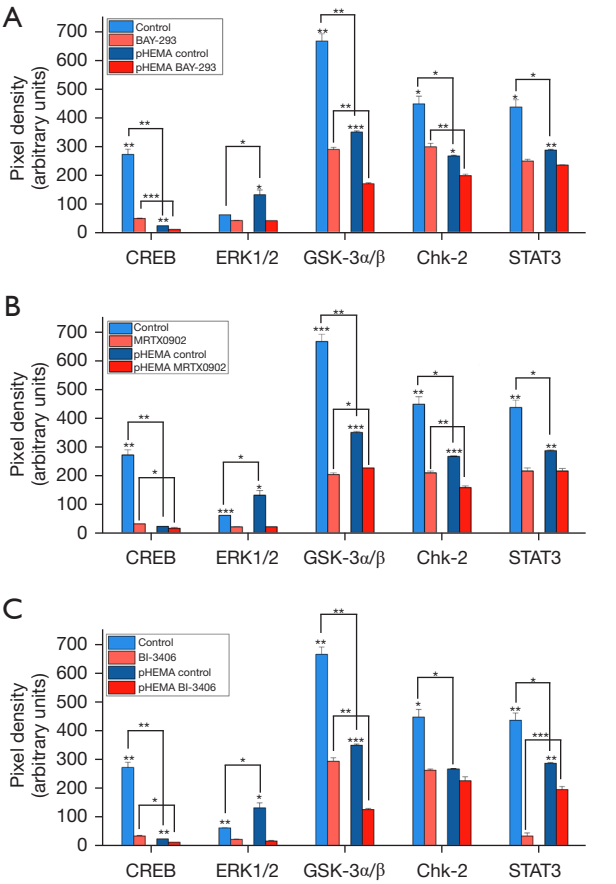

Figure 4 Comparison of the relative phosphorylation of proteins in BH1406 and BH1406 treated with 0.5 µM (A) BAY-293, (B) MRTX0902 and 0.2 µM (C) BI-3406 in addition to comparison between BH1406 and BH1406 pre-cultured on 6-well plates coated with pHEMA. Relative phosphorylation was determined by a Proteome Profiler Human Phospho-Kinase Array Kit (ARY003C, R&D Systems, Minneapolis, MN, USA). Data shown are mean values ± SD (*, P<0.05; **, P<0.01; ***, P<0.001). This figure shows CREB, ERK 1/2, GSK-3α/β, Chk-2 and STAT3.

phosphorylation of ERK 1/2.

STAT3 revealed a significantly decreased phosphorylation in pHEMA-cultivated BH1406 cells but still showed a diminished phosphorylation in response to all three SOS1 inhibitors with a major effect of BI-3406 in 2D cultures (*Figure 4A-4C*).

We tested the GSK-3 inhibitors CHIR-98014 and BI-5521, as well as the PI3K inhibitor dactolisib as a single drug and in combination with SOS1 inhibitor BAY-293 on 2D cells due to BH1406 revealing a high GSK-3α/β phosphorylation in Phospho-Kinase arrays (*Figures 4-7*). A combination of dactolisib with BAY-293 revealed synergistic effects between 10 and 0.63 µM (*Figure 5*). When BAY-293 was combined with BI-5521 a synergism from 10 to 0.0782 µM could be observed (*Figure 6*). A combination of BAY-293 with the GSK-3 inhibitor CHIR-98014 showed synergistic effects at 0.16 and 0.08 µM, respectively (*Figure 7*).

The BET-PROTAC ARV-771 was tested due to a high phosphorylation of ERK 1/2 in BH1406 (*Figures 4,8*). It exhibited synergism from 1.25 to 0.078 µM (*Figure 8*).

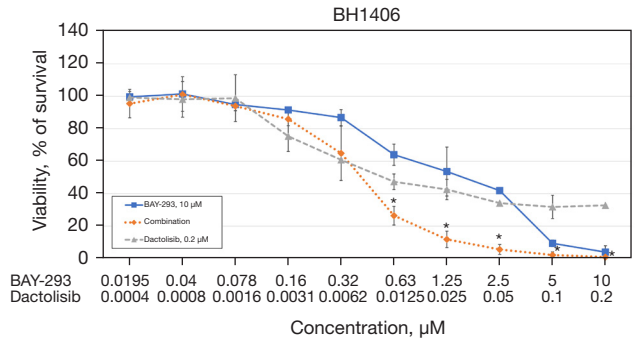

Figure 5 Cytotoxicity of BAY-293 (10 µM), dactolisib (0.2 µM) and their combination against 2D BH1406 evaluated via cytotoxicity assays. Data shown are mean values ± SD for 10 two-fold dilutions of the compounds and their combination. IC50-values are 1.53 µM for BAY-293, 0.54 µM for dactolisib and 0.42 µM for their combination. A combination of BAY-293 and dactolisib shows synergism from 10 to 0.63 µM, marked by an *. SD, standard deviation; IC50, half maximal inhibitory concentration.

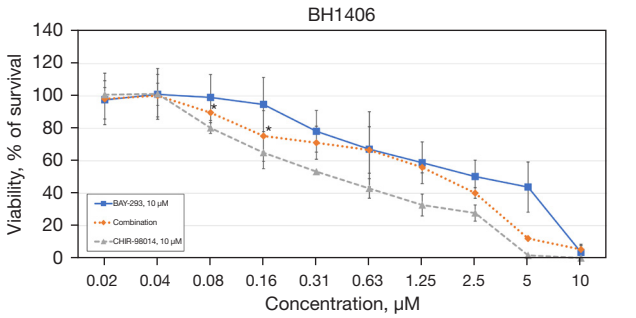

Figure 7 Cytotoxicity of BAY-293 (10 µM), CHIR-98014 (10 µM) and their combination against 2D BH1406 evaluated via cytotoxicity assays. Data shown are mean values ± SD for 10 two-fold dilutions of the compounds and their combination. IC50-values are 2.5 µM for BAY-293, 0.4 µM for CHIR-98014 and 1.71 µM for their combination. A combination of BAY-293 and CHIR-98014 shows synergism from 0.16 to 0.08 µM, marked by an *. SD, standard deviation; IC50, half maximal inhibitory concentration.

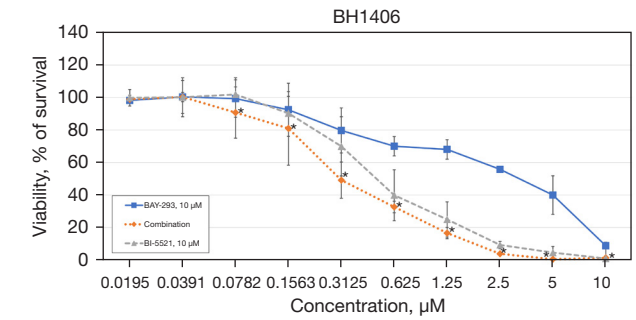

Figure 6 Cytotoxicity of BAY-293 (10 µM), BI-5521 (10 µM) and their combination against 2D BH1406 evaluated via cytotoxicity assays. Data shown are mean values ± SD for 10 two-fold dilutions of the compounds and their combination. IC50-values are 3.41 µM for BAY-293, 0.8 µM for BI-5521 and 0.31 µM for their combination. A combination of BAY-293 and BI-5521 shows synergism from 10 to 0.0782 µM, marked by an *. SD, standard deviation; IC50, half maximal inhibitory concentration.

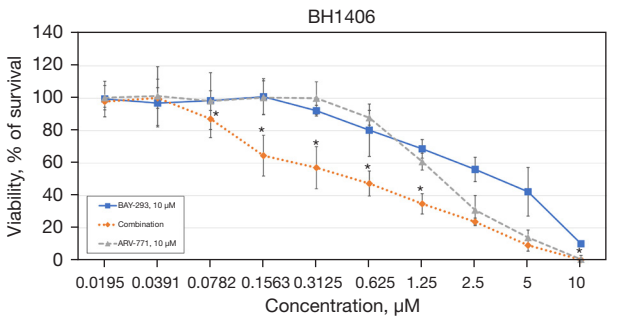

Figure 8 Cytotoxicity of BAY-293 (10 µM), ARV-771 (10 µM) and their combination against 2D BH1406 evaluated via cytotoxicity assays. Data shown are mean values ± SD for 10 two-fold dilutions of the compounds and their combination. IC50-values are 3.57 µM for BAY-293, 1.67 µM for ARV-771 and 0.53 µM for their combination. A combination of BAY-293 and ARV-771 shows synergism from 1.25 to 0.078 µM, marked by an *. SD, standard deviation; IC50, half maximal inhibitory concentration.

Discussion

Here we show that the NSCLC cell line BH1406 contains a rare SOS1 mutation and is sensitive to three distinct SOS1 inhibitors. Notably, no significant genomic alteration was detected in BH1406 parental tumor using routine Oncomine Focus Assay—NGS panel covering 52 most frequently mutated genes in lung cancer. The oncogenic activity of SOS1 in BH1406 was suggested based on functional screening and WES which are not implemented in lung cancer diagnostics.

The results suggest that the proliferation of the NSCLC cell line BH1406 is driven by the activating SOS1 mutation P481delinsLFFL. This mutation seems to be similar to the SOS1 P478L mutation described previously as oncogenic, except for the shifting of a nucleotide triplet (2). The BH1406 cell line has been detected using functional

screening of the pleura-derived cells using the SOS1 inhibitor BAY-293 (unpublished observation). No KRAS mutation was reported for this cell line. Son of Sevenless (SOS) was discovered in Drosophila melanogaster and found to be crucial for regular eye development (30). In humans, SOS has two homologues, namely SOS1 and SOS2. SOS1 encodes for the Son of Sevenless 1 protein which is a RAS GEF and putative RAC GEF. It can be activated by RAS by interaction with the allosteric binding site, thus relieving SOS1 autoinhibition (31). RAS^{GTP} binding increases SOS1 catalytic activity by up to 500-fold, setting up a RAS^{GTP}-SOS1-WT RAS positive feedback loop.

In a screen of genomes of 810 primary malignancies, missense SOS1 mutations were identified in a single pancreatic tumor, one lung adenocarcinoma, and a T-cell acute lymphoblastic leukemia cell line (32). Furthermore, reanalysis of 7,362 cancer exomes identified activating SOS1 mutations associated with NS as significantly altered in melanoma (33). For 26/7,362 tumors, a N233Y/I and 4 R552K/S mutations were detected revealing a significant overlap with some NS disease genes thus providing first evidence of somatic mutations of *SOS1* in melanoma. 22 of 129 NS patients did not display *KRAS* or *PTPN11* mutations (17%), however exhibited missense mutations in *SOS1* that do not overlap with the oncogenic SOS1 mutations (2). SOS1 mutations cluster at residues implicated in the maintenance of SOS1 in its autoinhibited form and ectopic expression of two NS-associated mutants elevated RAS activation. In summary, SOS1 is altered in 1.78% of all cancers with lung, colon, endometrial endometrioid adenocarcinoma, cutaneous melanoma, and breast invasive ductal carcinoma having the greatest prevalence of alterations (34).

SOS1 is a highly conserved GEF with multiple domains, including the DH, PH, REM, and CDC25 domains. The catalytic activity of SOS1 towards RAS is driven by its CDC25 and REM domains. Meanwhile, the histone fold DH/PH domains work together to promote the GTP/GDP exchange for RAC (5,6). The H, DH, and PH domains create an autoinhibitory module that obstructs the allosteric REM domain. This blockage prevents the activation of the catalytic CDC25 domain, ultimately inhibiting the function of SOS1 (2). One mechanism for SOS1 growth stimulation is the PIP2 membrane tethering via the SOS1 PH domain (35,36). Localization at the membrane facilitates the release of SOS1's autoinhibitory domain, initiating subsequent signaling pathways. The N233Y SOS1 mutant protein may show higher membrane affinity than the wild-type SOS1, enhancing the activation of KRAS and MYC target proteins. This supports SOS1's role in regulating RAS activity and MYC protein stability (10,11). Cells expressing multiple SOS1 mutations, such as the recurrent N233Y mutation, D309Y, P478L, and G604V mutations, showed a 48- to 100-fold increase of the formation of colonies in soft agar (2). These results suggest that mutated SOS1 carrying N233Y, D309Y, P478L, and G604V mutations functions as a proto-oncogene. Cells harboring the SOS1 N233Y mutant exhibited the most rapid growth, with tumors manifesting ten days after injection. Other tested SOS1 mutants also developed tumors, but these appeared more slowly, between 19 to 23 days after injection.

KRAS G12C, the mutation most commonly found in lung cancer, is addressed by specific drugs like sotorasib and adagrasib. However, other mutated alleles, frequently seen in pancreatic and colon cancers might be targeted indirectly through strategies that involve inhibiting SOS1, which is responsible for activating KRAS. Initial discoveries of SOS1 modulators revealed that they functioned as agonists, identifying a hydrophobic pocket within the catalytic site (19). High throughput screenings led to the identification of SOS1 inhibitors BAY-293 and BI-3406, both feature amino quinazoline scaffolds, which have been optimized with various substituents to enhance binding to the pockets (37). An initial inhibitor, BI-1701963 is currently undergoing clinical studies, where it is being tested both as a standalone treatment and in combination with a MAPK inhibitor or chemotherapy agents (38). SOS1 is a principal GEF for canonical RAS GTPases and activates RAS signaling (38). The development of novel SOS1 inhibitors, including BI-3406, BI-1701963 and MRTX0902, presents a potential therapy for SOS1-driven cancers. Out of the 11 cancer cell lines with SOS1 mutations and no concurrent RAS mutations, 10 demonstrated sensitivity to SOS1 inhibition in both 2D and 3D cell culture environments (39). *In vivo*, SOS1 inhibitors suppressed tumor growth in xenograft models of SOS1-mutant AML and NSCLC. Thus, our results suggest that SOS1 inhibition could be an effective therapeutic approach in RAS wild-type cancer patients with SOS1 mutations.

Our results demonstrate that the parent BH1406 is driven by an activating SOS1 mutation, and this patient may have profited from treatment with the cognate SOS1 inhibitors, alone or in combination with the PI3K inhibitor dactolisib, the GSK-3 inhibitor BI-5521 or the BET-directed PROTAC ARV-771 that impair downstream signal transduction and tumor proliferation. In general,

the SOS1 inhibitors exert larger effects in 3D cultures, most likely due to the increased activity of the signal transduction proteins ERK1/2 under 3D growth conditions. Downregulation of SOS1 demonstrates an additional effect of the SOS1 inhibitor BAY-293 and downregulation of MYC as the terminal target of the KRAS signaling proves the antiproliferative effect of this SOS1 inhibitor. In phosphoprotein arrays we found a downregulation of CREB, GSK-3α/β and CHK2 and, correspondingly, inhibitors directed to these proteins were found to synergize with the SOS1 inhibitor BAY-293.

In absence of any definite NGS standard array diagnosis the patient received chemotherapy with a dismal outcome. Even extended NGS diagnostic panels may not cover all of the possibly oncogenic SOS1 mutations. Up to 30% of all NSCLC patients lack an oncogenic driver and, at least, WES has to be performed to find drivers or combinations of genomic alterations that are responsible for the enhanced proliferation.

Conclusions

Some rare mutations in NSCLC oncogenic drivers are not included in routine diagnostic NGS panels covering the most frequent genetic alterations that can be tackled by approved therapeutics. Detection by functional inhibitor screening has the advantage to identify active agents but is restricted to the availability of sufficient numbers of viable tumor cells, in the case of NSCLC most easily from pleural effusions. For patients lacking detectable driver mutations, WES may be performed, and this method is more accessible nowadays due to reduced costs of this test.

Acknowledgments

Funding: None.

Footnote

Reporting Checklist: The authors have completed the MDAR reporting checklist. Available at https://tlcr.amegroups.com/article/view/10.21037/tlcr-24-570/rc

Data Sharing Statement: Available at https://tlcr.amegroups.com/article/view/10.21037/tlcr-24-570/dss

Peer Review File: Available at https://tlcr.amegroups.com/article/view/10.21037/tlcr-24-570/prf

Conflicts of Interest: All authors have completed the ICMJE uniform disclosure form (available at https://tlcr.amegroups.com/article/view/10.21037/tlcr-24-570/coif). G.H. serves as an unpaid editorial board member of *Translational Lung Cancer Research* from September 2023 to August 2025. The other authors have no conflicts of interest to declare.

Ethical Statement: The authors are accountable for all aspects of the work in ensuring that questions related to the accuracy or integrity of any part of the work are appropriately investigated and resolved. This study was conducted according to the Declaration of Helsinki (as revised in 2013). The study was approved by the Ethics Committee of the Medical University of Vienna, Vienna, Austria (Ethics Approval EK-21-210-1221) and informed consent of the patients was obtained from all individual participants.

References

1. Chevallier M, Borgeaud M, Addeo A, et al. Oncogenic driver mutations in non-small cell lung cancer: Past, present and future. World J Clin Oncol 2021;12:217-37.
2. Cai D, Choi PS, Gelbard M, et al. Identification and Characterization of Oncogenic SOS1 Mutations in Lung Adenocarcinoma. Mol Cancer Res 2019;17:1002-12.
3. Campbell JD, Alexandrov A, Kim J, et al. Distinct patterns of somatic genome alterations in lung adenocarcinomas and squamous cell carcinomas. Nat Genet 2016;48:607-16.
4. Sanchez-Vega F, Mina M, Armenia J, et al. Oncogenic Signaling Pathways in The Cancer Genome Atlas. Cell 2018;173:321-337.e10.
5. Rogge RD, Karlovich CA, Banerjee U. Genetic dissection of a neurodevelopmental pathway: Son of sevenless functions downstream of the sevenless and EGF receptor tyrosine kinases. Cell 1991;64:39-48.
6. Simon MA, Bowtell DD, Dodson GS, et al. Ras1 and a putative guanine nucleotide exchange factor perform

crucial steps in signaling by the sevenless protein tyrosine kinase. Cell 1991;67:701-16.
7. Chen PC, Wakimoto H, Conner D, et al. Activation of multiple signaling pathways causes developmental defects in mice with a Noonan syndrome–associated Sos1 mutation. J Clin Invest 2010;120:4353-65.
8. Nimnual AS, Yatsula BA, Bar-Sagi D. Coupling of Ras and Rac guanosine triphosphatases through the Ras exchanger Sos. Science 1998;279:560-3.
9. Sondermann H, Soisson SM, Boykevisch S, et al. Structural analysis of autoinhibition in the Ras activator Son of sevenless. Cell 2004;119:393-405.
10. Marampon F, Ciccarelli C, Zani BM. Down-regulation of c-Myc following MEK/ERK inhibition halts the expression of malignant phenotype in rhabdomyosarcoma and in non muscle-derived human tumors. Mol Cancer 2006;5:31.
11. Sears R, Leone G, DeGregori J, et al. Ras enhances Myc protein stability. Mol Cell 1999;3:169-79.
12. Allanson JE. Noonan syndrome. J Med Genet 1987;24:9-13.
13. Noonan JA. Noonan syndrome. An update and review for the primary pediatrician. Clin Pediatr (Phila) 1994;33:548-55.
14. Tartaglia M, Gelb BD. Disorders of dysregulated signal traffic through the RAS-MAPK pathway: phenotypic spectrum and molecular mechanisms. Ann N Y Acad Sci 2010;1214:99-121.
15. Tartaglia M, Pennacchio LA, Zhao C, et al. Gain-of-function SOS1 mutations cause a distinctive form of Noonan syndrome. Nat Genet 2007;39:75-9.
16. Roberts AE, Araki T, Swanson KD, et al. Germline gain-of-function mutations in SOS1 cause Noonan syndrome. Nat Genet 2007;39:70-4.
17. Lepri F, De Luca A, Stella L, et al. SOS1 mutations in Noonan syndrome: molecular spectrum, structural insights on pathogenic effects, and genotype-phenotype correlations. Hum Mutat 2011;32:760-72.
18. Hart TC, Zhang Y, Gorry MC, et al. A mutation in the SOS1 gene causes hereditary gingival fibromatosis type 1. Am J Hum Genet 2002;70:943-54.
19. Hillig RC, Bader B. Targeting RAS oncogenesis with SOS1 inhibitors. Adv Cancer Res 2022;153:169-203.
20. Zare M, Bigham A, Zare M, et al. pHEMA: An Overview for Biomedical Applications. Int J Mol Sci 2021;22:6376.
21. Benjamin D, Sato T, Cibulskis K, et al. Calling Somatic SNVs and Indels with Mutect2. bioRxiv 2019. doi: https://doi.org/10.1101/861054.
22. Kim S, Scheffler K, Halpern AL, et al. Strelka2: fast and accurate calling of germline and somatic variants. Nat Methods 2018;15:591-4.
23. Lai Z, Markovets A, Ahdesmaki M, et al. VarDict: a novel and versatile variant caller for next-generation sequencing in cancer research. Nucleic Acids Res 2016;44:e108.
24. McLaren W, Gil L, Hunt SE, et al. The Ensembl Variant Effect Predictor. Genome Biol 2016;17:122.
25. Richards S, Aziz N, Bale S, et al. Standards and guidelines for the interpretation of sequence variants: a joint consensus recommendation of the American College of Medical Genetics and Genomics and the Association for Molecular Pathology. Genet Med 2015;17:405-24.
26. Sondka Z, Bamford S, Cole CG, et al. The COSMIC Cancer Gene Census: describing genetic dysfunction across all human cancers. Nat Rev Cancer 2018;18:696-705.
27. Hillig RC, Sautier B, Schroeder J, et al. Discovery of potent SOS1 inhibitors that block RAS activation via disruption of the RAS-SOS1 interaction. Proc Natl Acad Sci U S A 2019;116:2551-60.
28. Hofmann MH, Gmachl M, Ramharter J, et al. BI-3406, a Potent and Selective SOS1-KRAS Interaction Inhibitor, Is Effective in KRAS-Driven Cancers through Combined MEK Inhibition. Cancer Discov 2021;11:142-57.
29. Ketcham JM, Haling J, Khare S, et al. Design and Discovery of MRTX0902, a Potent, Selective, Brain-Penetrant, and Orally Bioavailable Inhibitor of the SOS1:KRAS Protein-Protein Interaction. J Med Chem 2022;65:9678-90.
30. Pierre S, Bats AS, Coumoul X. Understanding SOS (Son of Sevenless). Biochem Pharmacol 2011;82:1049-56.
31. Margarit SM, Sondermann H, Hall BE, et al. Structural evidence for feedback activation by Ras.GTP of the Ras-specific nucleotide exchange factor SOS. Cell 2003;112:685-95.
32. Swanson KD, Winter JM, Reis M, et al. SOS1 mutations are rare in human malignancies: implications for Noonan Syndrome patients. Genes Chromosomes Cancer 2008;47:253-9.
33. Zhao B, Pritchard JR. Inherited Disease Genetics Improves the Identification of Cancer-Associated Genes. PLoS Genet 2016;12:e1006081.
34. AACR Project GENIE: Powering Precision Medicine through an International Consortium. Cancer Discov 2017;7:818-31.
35. Gureasko J, Galush WJ, Boykevisch S, et al. Membrane-dependent signal integration by the Ras activator Son of sevenless. Nat Struct Mol Biol 2008;15:452-61.

36. Zhao C, Du G, Skowronek K, et al. Phospholipase D2-generated phosphatidic acid couples EGFR stimulation to Ras activation by Sos. Nat Cell Biol 2007;9:706-12.
37. Hamilton G, Stickler S, Rath B. Targeting of SOS1: from SOS1 Activators to Proteolysis Targeting Chimeras. Curr Pharm Des 2023;29:1741-6.
38. Hofmann MH, Gerlach D, Misale S, et al. Expanding the Reach of Precision Oncology by Drugging All KRAS Mutants. Cancer Discov 2022;12:924-37.
39. Sale MJ, Mukherjee N, Ruzicka R, et al. SOS1 inhibition is an effective therapeutic strategy in SOS1-mutant cancer. Cancer Res 2023;83:abstr 1715.

Cite this article as: Hamilton G, Stickler S, Ermakov M, Eggerstorfer MT, Nocera FP, Hohenegger M, Weigl L, Hochmair MJ, Kashofer K. Characterization of the BH1406 non-small cell lung cancer (NSCLC) cell line carrying an activating SOS1 mutation. Transl Lung Cancer Res 2024;13(11):2987-2997. doi: 10.21037/tlcr-24-570

